High resolution photoassociation spectra of an ultracold Cs_2 long-range 0_u^+ $(6S_{1/2} + 6P_{1/2})$ state*

Chen Peng(陈 鹏), Li Yu-Qing(李玉清), Zhang Yi-Chi(张一驰), Wu Ji-Zhou(武寄洲), Ma Jie(马 杰)†, Xiao Lian-Tuan(肖连团), and Jia Suo-Tang(贾锁堂)

State Key Laboratory of Quantum Optics and Quantum Optics Devices, Laser Spectroscopy Laboratory, Shanxi University, Taiyuan 030006, *China*

(Received 25 March 2013; revised manuscript received 30 May 2013)

In this paper, ultracold cesium molecules are formed through photoassociation technology, which is carried out in a magneto-optical trap. High resolution photoassociaion spectra with the rotational progressions up to $J = 7$ are obtained. Three rovibrational levels of the long-range 0_u^+ state of Cs_2 below the $(6S_{1/2} + 6P_{1/2})$ dissociation limit are specifically investigated. By fitting their binding energy intervals to the non-rigid rotational model, the rotational constant of the long-range 0_u^+ state is determined. A proportional dependence of the value of the rotational constant on the vibrational quantum number is demonstrated.

Keywords: ultracold molecules, photoassociation, trap-loss spectrum, long-range molecular coefficient

PACS: 33.20.Vq, 33.15.Pw, 31.10.+z **DOI:** 10.1088/1674-1056/22/9/093301

1. Introduction

Recently, ultracold molecules have drawn great attention in physical research. Molecular gases refrigerated to the ultracold regime (< 1 mK) provide significant applications in molecular optics,[1,2] ultrahigh resolution spectroscopy,[3] ultracold chemistry,[4] and fundamental physical research.[5] Original insights stemming from cold and ultracold molecules have gradually focused on the quantum dynamics of complex systems and quantum information processing.[6] Nevertheless, even the simplest diatomic molecule has a complicated energy level structure compared to an atom due to the rich vibrational and rotational degrees of freedom. Thus the direct laser cooling of molecules seems out of reach. Interestingly, laser cooling of polar molecule SrF has been experimentally realized, reaching a few mK.[7] It should be noted that this route is only limited to specific large chemical molecules. Efficient and versatile approaches to producing ultracold molecules are still under exploration. Over the last decade, researchers have developed various methods to directly cool the molecules to lower temperatures, which mainly fall into two strategies, including imbedding and cooling molecules in a cryogenically cold buffer gas[8,9] and slowing molecular beams by Stark deceleration via an inhomogeneous electric field,[10,11] a supersonic jet,[12] or travelling optical lattices in intense optical fields.[13–15] Other techniques proposed theoretically include the sympathetic cavity cooling technique within a high-Q cavity[16] and ultrashort laser pulse induced photoassociation.[17,18] Molecular species obtained through direct cooling reach temperatures range from 10 mK to 100 mK, which are sufficiently low to study precision measurements,[5] cold chemistry,[19] and collisional properties.[20,21]

Although methods to directly cool molecules have been explored, none of them have successfully reached a temperature below a few μK. Alternative routes to acquiring ultracold molecules of $\sim$ μK start from ultracold atoms and assemble them pairwise into bound cold molecules by magneto- or photo-association (PA), i.e., indirect cooling.[19] Magneto-association can be realized owing to the existence of the Feshbach resonances originating from the coupling between the initial free atomic scattering state and a bound molecular state.[20] Photo-association, on the other hand, occurs as binding two colliding cold atoms through the resonant absorption of a photon into an excited molecule, which is stabilized by the spontaneous emission.[21]

Compared to the magneto-association, the PA of ultracold alkali atoms has become a powerful and versatile tool to obtain tightly bound cold molecules whose excited state levels are crucial in exploring the long-range dipole–dipole interaction and determining the molecular constants and even further the potential curves.[22] PA has been successfully employed in the production of homo- or hetero-nuclear molecules, such as Cs_2[23,24] and RbCs,[25,26] in the lowest vibrational levels of the electronic ground states. Photo-association spectroscopy (PAS) of ultracold molecules with high resolution is thus a convenient and robust tool to acquire the full infor-

*Project supported by the National Basic Research Program of China (Grant No. 2012CB921603), the National High Technology Research and Development Program of China (Grant No. 2011AA010801), the National Natural Science Foundation of China (Grant Nos. 61008012 and 10934004), the International Science and Technology Cooperation Program of China (Grant No. 2001DFA12490), the Project for Excellent Research Team of the National Natural Science Foundation of China (Grant No. 61121064), and the New Teacher Fund of the Ministry of Education of China (Grant No. 20101401120004).

†Corresponding author. E-mail: mj@sxu.edu.cn

© 2013 Chinese Physical Society and IOP Publishing Ltd

mation mentioned above. The PAS has been applied to various atomic species and different mixed species.[27] Very recently, the PAS of a specified Cs_2 0_g^- state has been utilized to reach the absolute frequency stabilization of a diode laser.[28] Especially, the long-range rovibrational molecule coefficient can be deduced from the PAS and then the atomic scattering length can be measured.[29,30] The PAS will continue to be a significant tool for ultrahigh resolution measurement,[31] atom–molecular collision studies,[32,33] creating deeply bound ground molecules,[34,35] and quantum computing.[36]

Since the first observation of the PAS of ultracold Cs_2 below the dissociation limit ($6S_{1/2}$ + $6P_{3/2}$),[34] the reported experimental and theoretical studies on Cs_2 have mainly focused on the molecular vibrational levels. The PAS has been performed in ultracold cesium atomic clouds with red detunings as large as 51 cm^{-1} and 56 cm^{-1} below the cesium ($6S_{1/2}$ + $6P_{3/2}$,$6P_{1/2}$) dissociation limit using trap-loss fluorescence detection by Pichler *et al.*[29,30] Later the detection range of the PAS has been extended for as far as 80 cm^{-1} below the Cs ($6S_{1/2}$ + $6P_{3/2}$) dissociation limit with a detailed analysis of the spectra by using the well-known LeRoy–Bernstein formula.[37] In the PAS, the rich rotational progressions for a specified vibrational state enable an accurate determination of the rotational constant. The rotational constant for the Cs_2($6S_{1/2}$ + $6P_{3/2}$) 0_g^- state has been reported.[31,38,39] However, the rotational constant of the cesium molecular ($6S_{1/2}$ + $6P_{1/2}$) 0_u^+ state has not yet been presented. In this paper, the technique of modulated fluorescence of cold atoms in a cesium magneto-optical trap is employed to obtain the high resolution PA spectrum for the Cs_2 ($6S_{1/2}$ + $6P_{1/2}$) 0_u^+ state with rich rotational levels, according to which the rotational constants are obtained by using the LeRoy–Bernstein (LRB) formula as well as the non-rigid rotational model.

2. Experimental setup

The experiment was carried out in a conventional vapor cell loaded magneto-optical trap (MOT) where an ensemble of cesium atoms was prepared. As described in detail in Refs. [38]–[41], a number of cold atoms ($\sim 10^7$) were accumulated in the quartz vacuum chamber with a background pressure of about 10^{-7} Pa. The temperature of the cold atomic sample was $\sim$ 200 μK as measured by the time of flight method. The trapping and repumping lasers were provided by two frequency-stabilized diode lasers (DL100, linewidth < 1 MHz) via standard saturated absorption technology. The trapping laser frequency was red-detuned from the $6S_{1/2}$ ($F = 4$) $\rightarrow 6P_{3/2}$ ($F' = 5$) atomic transition for about two natural linewidths. The repumping laser was locked to the transition of $6S_{1/2}$ ($F = 3$) $\rightarrow 6P_{3/2}$ ($F' = 4$). The experimental setup is shown in Fig. 1.

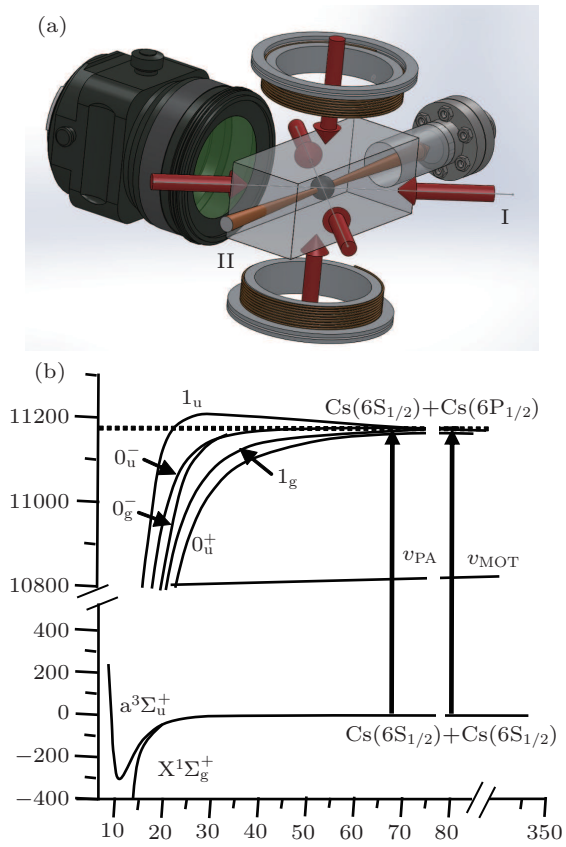


Fig. 1. (color online) (a) Experimental setup, where arrow I represents the trapping beam and the re-pump beam, and arrow II represents the PA laser; (b) relevant energy levels of Cs_2 molecule.

The photoassociation process was induced by a continue-wave tunable Ti: sapphire laser system (MBR 110, $\sim$ 900 mW, typical linewidth $<$ 100 kHz). The photoassociation laser beam was focused to a diameter of 500 μm at the center of the vacuum chamber, resulting in an available intensity of $\sim$ 300 W/cm^2. The absolute laser frequency was measured by using a commercial wavelength meter (High Finesse-Angstrom WS/7R) with an accuracy of 60 MHz, which enabled a comparatively accurate analysis of the spectral data. The fluorescence yielded from the trapped cold atoms was collected by a convex lens and detected by an avalanche photodiode (APD Hamamatsu S3884) with 850 nm band-pass filters. In order to improve the sensitivity of the detection, we utilized a lock-in detection technique by modulating the fluorescence of the cold atoms.[28,39] The modulated fluorescence signal was demodulated through a lock-in amplifier (SR830) with an optimized integration time of 300 ms.

In our experiment, trap-loss spectroscopy instead of the ionization detection technique was employed to detect the production of cesium molecules.[42] In the photoassociation process, a pair of cold atoms in the ground state ($6S_{1/2}$, $F = 4$) resonantly absorbed a photon whose frequency was red detuned from the ($6S_{1/2}$ + $6P_{3/2}$) dissociation limit, thus forming a weakly bound molecule residing in the excited state. The

process can be written as

$$\mathrm{Cs}(6\mathrm{S}_{1/2}) + \mathrm{Cs}(6\mathrm{S}_{1/2}) + \hbar\nu \rightarrow \mathrm{Cs}_2. \quad (1)$$

In the molecular forming process, the number of trapped cold atoms in the MOT decreased, and therefore the fluorescence from the atomic resonant transition between the ground state and the excited sate showed a loss, meaning that the excited bound molecule was formed.[37]

3. High sensitivity rovibrational spectra

For the long-range $(6\mathrm{S}_{1/2} + 6\mathrm{P}_{1/2})$ 0_u^+ state of Cs_2, the high resolution rotational spectra are shown in Fig. 2, and the rotational quantum number is resolved up to $J = 7$ for the vibrational state ($v = 214$). The spectra exhibit different narrow and strong resonance lines, which result from the variation of the Franck–Condon factors for the PA transitions from the initial state of the two cold free atoms to the final rovibrational levels of the long-range states.[39] Here the rotational quantum numbers are assigned in the spectra based on the accurate spectroscopic investigation.[43] For 0_u^+ state below the Cs_2 $(6\mathrm{S}_{1/2} + 6\mathrm{P}_{1/2})$ dissociation limit, the molecular levels tend to couple with the same symmetry belonging to the 0_u^+ state below the $(6\mathrm{S}_{1/2} + 6\mathrm{P}_{3/2})$ dissociation limit. It is worth noting that the coupling of these levels provides an alternative route to obtaining ultracold ground molecules.[35]

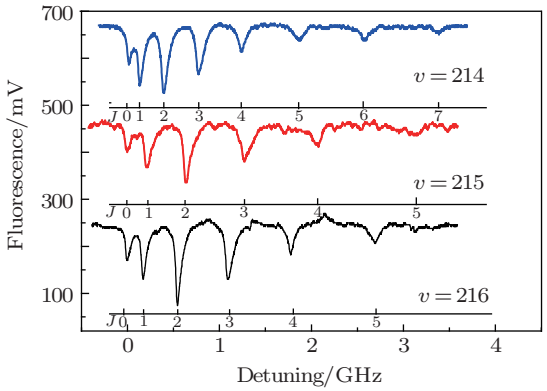


Fig. 2. (color online) Ultrahigh resolution PA spectra for $v = 214$, 215, 216 vibrational states of the Cs_2 long-range 0_u^+ state.

We demonstrate the high resolution rotational spectra for the vibrational levels $v = 214$, 215, 216, which are induced by using the Ti: sapphire laser as the photoassociation source, whose frequency is red detuned $\sim 47.96\ \mathrm{cm}^{-1}$, $\sim 49.33\ \mathrm{cm}^{-1}$, and $\sim 50.37\ \mathrm{cm}^{-1}$ from the Cs_2 $(6\mathrm{S}_{1/2} + 6\mathrm{P}_{1/2})$ dissociation limit, respectively. In the MOT, a comparatively low temperature of 100 μK is reached. The s-wave scattering scheme predominates the formed excited molecules at the rotational quantum level of $J = 2$, thus leading to a strong loss signal in this rotational progression for the three vibrational states, as shown in Fig. 2. We have observed 6 rotational levels for vibrational levels $v = 214$, 215, 216 with rotational quantum numbers from $J = 0$ to $J = 5$. All the observed spectra exhibit the same intensity undulation, owing to the variation of the Franck–Condon factors for the photoassociation transitions from the initial scattering state of the two cold free atoms to the final targeted rovibrational levels of the long-range states.[43] It should be noticed that for an additional $J = 6$, the 7th rotational level in $v = 214$ is detected. This is attributed to an additional angular momentum contribution, such as from the orbital angular moment due to p-wave or d-wave.[44]

4. Determination of rotational constant

In the experiment, trap loss spectra with large detunings below the $6\mathrm{P}_{1/2}$ dissociation limit were measured carefully. The spectra are of key importance in determining the molecular rotational constant. Specifically, it is interesting to note that we have observed the rotational levels of the Cs_2 molecular 0_u^+ state from $J = 0$ to $J = 5$ (or $J = 7$) for the molecular vibrational levels $v = 215$, 216, 214, which have not yet been reported to our knowledge. Furthermore, the presented results indicate that various partial wave scattering collisions have participated in the atom–atom collision.[45,46] For the long-range 0_u^+ state of Cs_2, the observed rotational quantum number J is given by $J = L + S + l$, where $L = 1$ is the total electronic orbital angular momentum, $S = 1$ is the total electronic spin momentum, and l is the magnitude of the orbital angular momentum of the collisional atomic pair. The rotational quantum number J satisfies the following formula:

$$|l - |L + s|| \leq J \leq |l + |L + s||. \quad (2)$$

Besides, the quantum numbers should meet the selection rule $J + L =$ even number, which is the result of the symmetry requirement for the two-body wave function.

In order to analyze the molecular rotational spectral data, we employ the relationship between binding energy and rotational quantum number

$$E/hc = BJ(J+1), \quad (3)$$

where E is the molecular rotational energy eigenvalue, h is the Planck constant, c is the speed of light, and B is the rotational constant in units of cm^{-1}. The above formula was obtained by considering a simple rigid rotation model in Ref. [45].

Compared with the conventional chemical bond, the long-range interaction between two alkali atoms of excited diatomic molecules formed by photoassociation is weak and the binding energy can be written by considering the nonrigid rotation model as

$$E/hc = BJ(J+1) - DJ^2(J+1)^2, \quad (4)$$

where D is the centrifugal distortion constant in units of cm^{-1}. The effect from the centrifugal distortion is significant for the

rotational levels with high rotational quantum numbers, because the electronic rotation at the higher rotational energy level with a higher angular velocity, whose direction is perpendicular to the molecular axis, tends to produce a more severe influence on the diatomic vibrational motion in the radial direction.

For the same vibrational quantum number, the interval ΔE between the neighboring rotational levels is

$$\Delta E = [E(J+1) - E(J)]/hc = 2B(J+1) - 4D(J+1)^3. \quad (5)$$

In order to consider the influence of the centrifugal distortion effect on the molecular vibrational progress, the centrifugal distortion constant D is introduced.[45] Figure 3 shows a good agreement between the high resolution molecular rotational data and the fitting of nonlinear equation (5), which contains the rotational constant B and the centrifugal distortion D, for the three molecular levels. The rotational constants, 0.00242 cm^{-1}, 0.00175 cm^{-1}, 0.0015 cm^{-1} for the three vibrational states, respectively, are obtained by fitting data to Eq. (5). The variations of the rotational constants with the molecular vibrational quantum number are presented in Fig. 3 and the constants are shown to increase as the vibrational number increases.

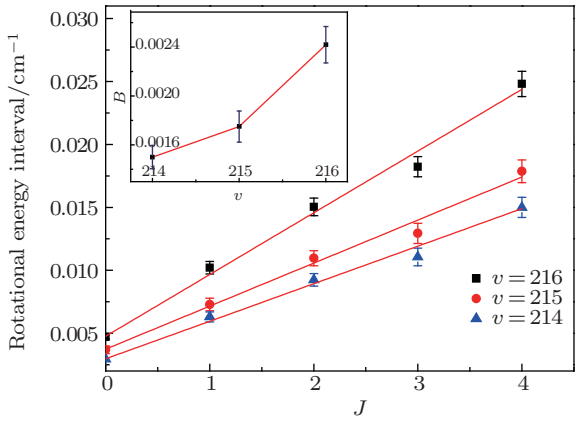


Fig. 3. (color online) Rotational energy level interval Δv versus rotational quantum number J for $v = 214$, 215, 216 of the Cs_2 long-range 0_u^+ state. The symbols represent experimental data, while the solid curves refer to the corresponding theoretical fitting according to Ref. [39]. The inset illustrates the dependence of rotational constant on vibrational quantum number v.

For the long-range state of a cesium dimer, the distance between two atoms tends to be large with vibrational number increasing, and the excited molecular state is closer to the dissociation limit. This results in the increase of the vibrational energy spacing while the vibrational number augments. It can be reasonably explained by the fact that a vibrational level contains many rotational levels; the rotational energy spacing contributes to the enhancement of the energy spacing and the rotational constant for the long-range 0_u^+ state of Cs_2 below the $(6S_{1/2} + 6P_{1/2})$ dissociation limit.

5. Conclusion

We experimentally present the rotational spectra with high resolution for the long-range 0_u^+ state of Cs_2 by modulating the fluorescence of the cold atoms. Three vibrational states of $v = 214$, 215, 216 are observed below the Cs_2 $(6S_{1/2} + 6P_{1/2})$ dissociation limit. The rotational constants for different vibrational states are derived by fitting experimental data to the nonrigid rotation model. The values of $B(v)$ for the above vibrational levels are equal to 0.00242 cm^{-1}, 0.00175 cm^{-1}, and 0.0015cm^{-1}, respectively. The dependence of the rotational constant on the vibrational quantum number is also studied.

References

[1] Dong G J, Edvadsson S, Lu W P and Barker P F 2005 *Phys. Rev. A* **72** R031605
[2] Gordon R J, Zhu L C, Schroeder W A and Seideman T 2003 *J. Appl. Phys.* **94** 669
[3] Ma J, Wang L R, Zhao Y T, Xiao L T and Jia S T 2009 *J. Mol. Spectrosc.* **255** 106
[4] Krems R V 2005 *Int. Rev. Phys. Chem.* **24** 99
[5] DeMille D, Sainis S, Sage J, Bergeman T, Kotochigova S and Tiesinga E 2008 *Phys. Rev. Lett.* **100** 043202
[6] Yelin S F, Kirby K and Côté R 2006 *Phys. Rev. A* **74** 050301
[7] Shuman E S, Barry J F and DeMille D 2010 *Nature* **467** 820
[8] Weinstein J D, DeCarvalho R, Guillet T, Friedrich B and Doyle J M 1998 *Nature* **395** 148
[9] Buuren L D, Sommer C, Motsch M, Pohle S, Schenk M, Bayerl J, Pinkse P W H and Rempe G 2009 *Phys. Rev. Lett.* **102** 033001
[10] Meerakker S Y, Smeets P H, Vanhaecke N, Jongma R T and Meijer G 2005 *Phys. Rev. Lett.* **94** 023004
[11] Van Veldhoven J, Bethlem H L and Meijer G 2005 *Phys. Rev. Lett.* **94** 083001
[12] Sawyer B C, Stuhl B K, Wang D, Yeo M and Ye J 2008 *Phys. Rev. Lett.* **101** 203203
[13] Fulton R, Bishop A I, Shneider M N and Barker P F 2006 *Nat. Phys.* **2** 465
[14] Dong G J, Lu W P and Barker P F 2004 *Phys. Rev. A* **69** 013409
[15] Dong G J, Lu W P, Barker P F and Shneider M N 2005 *Progress in Quantum Electronics* **29** 1
[16] Dong G J, Wang C and Zhang W P 2012 arxiv: **1205** 1876
[17] Lin F, Zhang W, Zhao Z Y and Cong S L 2012 *Chin. Phys. B* **21** 073203
[18] Li L, Niu Y Y, Yuan K J and Cong S L 2007 *Chin. Phys.* **16** 2957
[19] Carr L D, DeMille D, Krems R V and Ye J 2009 *New J. Phys.* **11** 055049
[20] Chin C, Grimm R, Julienne P and Tiesinga E 2010 *Rev. Mod. Phys.* **82** 1225
[21] Jones K M, Tiesinga E, Lett P D and Julienne P S 2006 *Rev. Mod. Phys.* **78** 483
[22] Dulieu O and Gabbanini C 2009 *Rep. Prog. Phys.* **72** 086401
[23] Viteau M, Chotia A, Allegrini M, Bouloufa N, Dulieu O, Comparat D and Pillet P 2008 *Science* **321** 232
[24] Zhang Yi C, Wu J Z, M J, Zh Y T, W L R, X L T and J S T 2010 *Acta Phys. Sin.* **59** 5418 (in Chinese)
[25] Sage J M, Sainis S, Bergeman T and DeMille D 2005 *Phys. Rev. Lett.* **94** 203001
[26] Yang Y, Ji Z H, Yuan J P, Wang L R, Zhao Y T, Ma J, Xiao L T and Jia S T 2012 *Acta Phys. Sin.* **61** 213301 (in Chinese)
[27] Jones K M, Tiesinga E, Lett P D and Julienne P S 2006 *Rev. Mod. Phys.* **78** 483
[28] Ma J, Wang L R, Zhao Y T, Xiao L T and Jia S T 2007 *Appl. Phys. Lett.* **91** 161101
[29] Pichler M, Chen H and Stwalley W C 2004 *J. Chem. Phys.* **121** 1796
[30] Pichler M, Chen H and Stwalley W C 2004 *J. Chem. Phys.* **121** 6779
[31] Drag C, Tolra B L, Dulieu O, Comparat D, Vatasescu M, Boussen S, Guibal S, Crubellier A and Pillet P 2000 *IEEE J. Quantum Electron.* **36** 1378

[32] Staanum P, Kraft S D, Lange J, Wester R and Weidemüller M 2006 *Phys. Rev. Lett.* **96** 023201

[33] Zahzam N, Vogt T, Mudrich M, Comparat D and Pillet P 2006 *Phys. Rev. Lett.* **96** 023202

[34] Fioretti A, Comparat D, Crubellier A, Dulieu O, Masnou-Seeuws F and Pillet P 1998 *Phys. Rev. Lett.* **80** 4402

[35] Dion C M, Drag C, Dulieu O, Laburthe Tolra B, Masnou-Seeuws F and Pillet P 2001 *Phys. Rev. Lett.* **86** 2253

[36] Chaudhury S, Merkel S, Herr T, Silberfarb A, Deutsch I H and Jessen P S 2007 *Phys. Rev. Lett.* **99** 163002

[37] Ma J, Wang L R, Zhao Y T, Xiao L T and Jia S T 2009 *J. Mol. Spectrosc.* **255** 106

[38] Wu J Z, Ma J, Ji Z H, Zhang Y C, Li Y Q, Wang L R, Zhao Y T, Chen G, Xiao L T and Jia S T 2012 *Chin. Phys. B* **21** 093701

[39] Ma J, Wu J Z, Zhao Y T, Xiao L T and Jia S T 2010 *Opt. Express* **18** 17089

[40] Ma J, Wang L R, Ji W B, Xiao L T and Jia S T 2007 *Chin. Phys. Lett.* **24** 1904

[41] Wu J Z, Ma J, Zhang Y C, Li Y Q, Wang L R, Zhao Y T, Chen G, Xiao L T and Jia S T 2011 *Phys. Chem. Chem. Phys.* **13** 18921

[42] Zhang H S, Ji Z H, Yuan J P, Zhao Y T, Ma J, Wang L R, Xiao L T and Jia S T 2011 *Chin. Phys. B* **20** 123702

[43] Wester R, Kraft S D, Mudrich M, Staudt M, Lange J, Vanhaecke N, Dulieu O and Weidemüller M 2004 *Appl. Phys. B* **79** 993

[44] Li Y Q, Ma J, Wu J Z, Zhang Y C, Zh Y T, W L R, Xiao L T and Jia S T 2012 *Chin. Phys. B* **21** 043404

[45] Gomez E, Black A T, Turner L D, Tiesinga E and Lett P D 2007 *Phys. Rev. A* **75** 013420

[46] Feng Z F, Li W D, Xiao L T and Jia S T 2009 *Chin. Phys. B* **18** 4901